Indium-free organic thin-film solar cells using a plasmonic electrode

Indium-free organic thin-film solar cells using a plasmonic electrode

Kentaro Takatori[1,2,3]**, Takayuki Nishino**[1,4]**, Takayuki Okamoto**[1,2,5]**,
Hiroyuki Takei**[6]**, Koji Ishibashi**[1,5] **and Ruggero Micheletto**[3]

[1] Advanced Device Laboratory, RIKEN, Hirosawa, Wako, Saitama 351-0198, Japan
[2] Interdisciplinary Graduate School of Science and Engineering, Tokyo Institute of Technology, Yokohama 226-8502, Japan
[3] Graduate School of Nanobioscience, Yokohama City University, Seto, Kanazawa-ku, Yokohama, Kanagawa 236-0027, Japan
[4] Sanwa Corporation, Izuka, Kumagaya, Saitama 360-0231, Japan
[5] RIKEN Center for Emergent Matter Science, Hirosawa, Wako, Saitama 351-0198, Japan
[6] Faculty of Life Science, Toyo University, Izumino, Itakura, Gunma 374-0913, Japan

E-mail: okamoto@riken.jp

Received 20 November 2015, revised 26 February 2016
Accepted for publication 1 March 2016
Published 7 April 2016

CrossMark

Abstract

We propose a new kind of organic solar cell (OSC) that substitutes the standard indium tin oxide (ITO) electrode with a silver layer with randomly arranged circular nanoholes (plasmonic electrode). The quasi-random structure in the silver layer efficiently converts wideband incident light into surface plasmon polaritons propagating along the surface of the silver film. In this way, the converted surface plasmon polaritons enhance light absorption in the active layer. We describe in detail the fabrication process we used and we give a thorough report of the resulting optical characteristics and performances. Although the transmittance of the plasmonic electrode is approximately one-third of that of the ITO electrodes, the power conversion efficiency of the OSCs with our plasmonic electrode is comparable to that of conventional inverted solar cells using ITO electrodes. Moreover, the obtained incident photon to current efficiency was better than that of the inverted solar cells in the wavelength regions around 400 nm and over 620 nm.

Keywords: surface plasmon, photovoltaic, organic materials

(Some figures may appear in colour only in the online journal)

1. Introduction

Organic thin-film solar cells (OSCs) are promising as renewable clean energy sources because of their potential for low-cost and high throughput processing [1–3]. In OSCs, indium tin oxide (ITO) is usually used as the material for the transparent electrodes [4]. Indium tin oxide exhibits high transparency in the visible range and high electrical conductivity. However, ITO has some drawbacks. It is expensive, since indium is a rare-metal and a strategic material [5]. Another problem is its low flexibility. Since ITO is a ceramic, it easily cracks and fractures with relatively low stress [6]. Microcracks drastically decrease the electrical conductance of ITO films [7]. Although other conductive metal oxides, such as zinc oxide and fluorine tin oxide, are being studied as the transparent electrode, their optical and electrical properties are still inferior to those of ITO [5, 8]. Carbon nanotube (CNT) and graphene are also studied as candidates for the transparent electrodes [5] in OSCs. While the mobility of CNT is high [9], the transmittance is low due to CNTs' high absorption and reflection in almost the entire visible and infrared regions [5]. Reducing the film thickness increases the transparency, but unfortunately decreases the electrical conductance and its homogeneity. Recently, graphene has drawn much attention as a next-generation transparent electrode due to its high mobility [10, 11] and transparency. The predicted optical and electrical properties of graphene film [12, 13] in theory are comparable to those of ITO, but experimentally the

J. Phys. D: Appl. Phys. **49** (2016) 185106

K Takatori *et al*
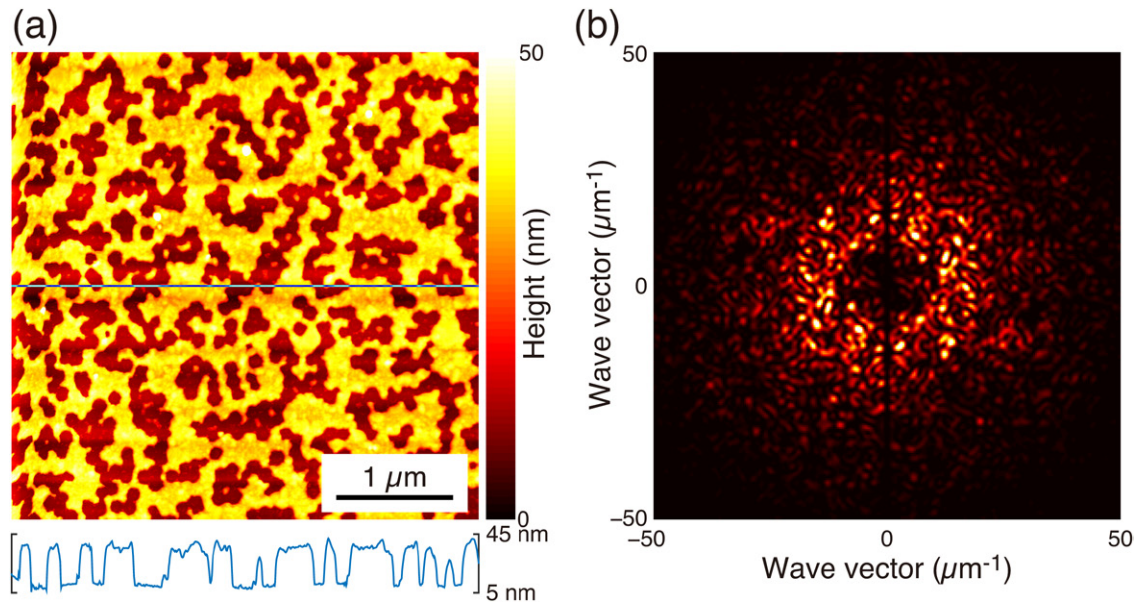
Figure 1. (a) AFM image of a 30 nm thick plasmonic electrode. Cross-sectional height distribution along the line shown in the image is also shown at the bottom. (b) Spatial frequency spectrum of (a).

obtained sheet resistance is higher than that of ITO [5, 14]. This suggests that it is still difficult to use graphene as a good transparent electrode for solar cells. Metal films are also candidates for a transparent electrode, but even metal films a few nanometers thick exhibit insufficient transparency [15, 16]. In addition, as the thickness of the metal film decreases, electron scattering from the surface and grain boundary dramatically decrease the conductance [17, 18].

An alternative idea to improve the transmittance of metal films is the perforation of nanoslits or nanoholes on them. Organic solar cells employing a 20–40 nm thick metal film with a nanostructure such as the transparent electrode has been proposed [19–24]. These structures carved on metal are called plasmonic structures, because surface plasmon polaritons (SPPs) are supported on such a metal surface. Obviously these apertures or slits enhance the transparency of metal films, while degrading their electric conductance [25, 26]. Since the transparency of patterned metal films is lower than that of ITO films, SPPs have to play an important role in OSCs. The plasmonic structure converts incident light into SPPs that propagate along the metal-dielectric interface. The converted surface plasmon polaritons are efficiently absorbed by the active layer of OSCs due to its long lifetime, resulting in the enhancement of the conversion efficiency [27–29].

If the goal is to replace the ITO layer, a structure that uses localised surface plasmons is not suitable, because localised surface plasmons are generated by metallic nanoparticles that exhibit no macroscopic conductivity unless they are aggregated. Thus, in this study we use instead a continuous metallic surface that allows the propagation of surface plasmons. Many kinds of OSCs boosted with propagating surface plasmons have been proposed so far [19–23]. In order to couple incident light to surface plasmons propagating along a metallic surface, one-dimensionally (1D) or two-dimensionally (2D) periodic perforation [19–22] is often employed. However, since these structures have only one or two reciprocal lattice vectors, only a

few wavelength components of the incident light are converted to SPPs when the angle of incidence is fixed. Additionally, 1D periodic structures exhibit a strong polarization dependency, resulting in low conversion efficiency. In order to eliminate dependence on the incident angle and the polarisation for the efficient excitation of SPPs, random structures are more suitable. Reilly *et al* proposed silver thin-films with randomly perforated circular nanoholes [23, 24]. Their proposed random structure has no polarization dependence in the excitation of SPPs. However, since all nanoholes are identical in shape and they are isolated from each other, the spectral bandwidth of their structure is not so wide [24]. For broadening the spectral response, Stec and Hatton [30] proposed thin metal films with nanoholes with a random shape, for which structure they control the adhesion of the metal film to substrates. In this paper, we propose an improved nanostructure, where a thin silver film with circular nanoholes are arranged in non-constrained random positions. In this way the resulting structure has holes that have mixed shapes, single isolated circles and different random shapes made by one or more circles merged with each other. The obtained plasmonic electrode provides a wider spectral response than those previously proposed electrodes [24], presents no polarisation dependence and is also suitable for flexible devices. Hereafter we describe in detail the optical and electrical properties of these novel plasmonic electrodes; we also constructed conventional standard OSCs in which the ITO electrode is replaced with this original plasmonic one and fully evaluate their characteristics.

2. Plasmonic electrodes and their optical and electrical properties

Figure 1(a) shows an atomic force micrograph (AFM) of the plasmonic electrode we fabricated. The diameter of the holes is 100 nm with a coverage of ∼30%. Figure 1(b) shows the spatial frequency spectrum of the plasmonic electrode shown

Table 1. Characteristics of the plasmonic solar cells and the inverted ones.

	V_{oc} (mV)	J_{sc} (mA cm^{-2})	FF (%)	PCE (%)
Plasmonic solar cell	554 ± 4.88	7.26 ± 0.896	55.6 ± 3.25	2.23 ± 0.203
Inverted-type solar cell	541 ± 20.8	9.20 ± 0.681	48.3 ± 2.41	2.41 ± 0.325

in figure 1(a). The spectrum is isotropic and has a wideband, which contributes to converting wideband sunlight into SPPs propagating along the surface of the plasmonic electrode. The wide bandwidth of our proposed structure comes from the arrangement of the nanoholes. Unlike the structures proposed by Reilly *et al* [23, 24], in our structure the nanoholes form chain-like clusters and the shapes are no longer circular.

A colloidal lithography methodology was used to fabricate the plasmonic electrodes. A 1 mm thick glass substrate was immersed in an aqueous solution of 3-aminopropyltrimethoxysilane (1 wt%) for 1 min to promote the subsequent binding of silica nanospheres onto the glass surface. After washing with deionised water, the substrate was dried in an oven at 50 °C, and then immersed in a 2.5% aqueous suspension of silica nanospheres 100 nm in diameter (polysciences) for 1 min. After rinsing with water to remove the excess nanospheres, the substrate was dried in the oven at 50 °C. Then a silver film of 10, 20, 30 or 40 nm was evaporated onto the substrate. Finally, we removed the particles with scotch tape to complete the fabrication process. The AFM image shows that all of the particles are completely removed by the scotch tape and no tape glue remains. The use of scotch tape for removing particles provides good reproducibility. This fact can be confirmed from table 1, as will be shown later. The obtained standard deviations are comparable to those for the solar cells with an ITO electrode.

Figure 2(a) shows the thickness dependence of the sheet resistance of our plasmonic electrodes compared with plane silver thin films. For further comparison, the sheet resistance of 100 nm thick ITO films is also shown. Although the sheet resistance of the plasmonic electrodes was higher than that of the plane silver films with the same thickness, the sheet resistance of the 30 nm thick plasmonic electrodes resulted in being comparable to that of the ITO films. The measured transmittance, reflectance and absorptance spectra of a 30 nm thick plasmonic electrode on a glass substrate and a 30 nm thick plane silver film on the same glass substrate are shown in figures 2(b) and (c), respectively. The transmittance of the plane silver film at a 500 nm wavelength was only 23%, whereas that of the plasmonic electrode was 35%. In addition to the enhancement of the transmittance, the absorptance was also enhanced by introducing the above described nanoholes. In this way, the absorptance of the plasmonic electrode increased from 19% to 51% at a 500 nm wavelength. The absorption enhancement is caused by the excitation of long-lived SPPs by the silver film, since there are no other absorption media. In actual solar cells, however, the SPPs are absorbed mainly by the active materials, because these have a high absorption coefficient and most of the SPP field lies within the dielectric media [29, 31].

3. Fabrication of plasmonic solar cells

We fabricated inverted OSCs in which the ITO electrode is replaced by the plasmonic electrode described above. Hereafter, we call these solar cells plasmonic solar cells. Figure 3 shows the layer structure of the plasmonic solar cell compared with a conventional inverted solar cell with an ITO electrode. Both solar cells consist of a glass substrate that holds the following layer structure: a plasmonic electrode or an ITO electrode / TiO$_2$ / poly(3-hexylthiophene): [6, 6]-phenyl C_{61} butyric acid methyl ester (P3HT:PCBM) / MoO$_3$ / silver. The plasmonic electrode was made 30 nm thick after considering a trade-off between the optical and electric properties. The thickness of the TiO$_2$ layer in the inverted solar cells was 7 nm, which was optimal for power conversion efficiency (PCE) in the conventional OSCs. On the other hand, the obtained short-circuit current of the plasmonic solar cells with a 7 nm thick TiO$_2$ layer was very low. This may have been caused by the surface roughness of the plasmonic electrode. A 7 nm thick TiO$_2$ layer may be too thin to cover the plasmonic electrode completely. We employed a 26 nm thick TiO$_2$ layer, which exhibited the best performance in the plasmonic solar cells. The thicker TiO$_2$ layer does not affect the transmission of incident light because of the high transparency of TiO$_2$ in the visible range. The thicknesses of the other layers are identical in both solar cells.

The fabrication procedure is as follows: first, TiO$_2$ was sputtered on the ITO electrode or on the plasmonic electrode. Then we prepared the P3HT:PCBM solution by dissolving 15 mg P3HT and 15 mg PCBM into 1 mL 1,2-dichlorobenzene. The mixture was stirred at 100 °C for 24 h in a nitrogen atmosphere. Then, it was spin-coated onto the TiO$_2$ layer. The film thickness of the P3HT:PCBM layer was ∼150 nm. The devices were not intentionally but naturally annealed. Finally, a 10 nm thick MoO$_3$ layer and a 100 nm thick silver back electrode were deposited onto the devices with thermal evaporation.

4. Results and discussion

Figure 4(a) shows the measured I–V characteristics of the plasmonic solar cells and the inverted solar cells under simulated AM 1.5 solar illumination (100 mW cm^{-2}). Table 1 summarises the I–V characteristics of both cells. The obtained PCE and short-circuit current density, J_{sc}, of the plasmonic solar cells were lower than those of the inverted ones, whereas the fill factor (FF) of the plasmonic solar cells was higher than that of the inverted ones. The open-circuit voltage, V_{oc}, of the plasmonic solar cells was almost the same as that of the inverted ones. Although the transmittance of the plasmonic electrode is only one third of that of the ITO, the obtained PCE of the plasmonic solar cells is comparable to that of the inverted ones. This result indicates that the SPPs excited in the plasmonic electrodes give an important contribution to the current generation. The higher FF has a role in the improvement of the PCE of our cells. The higher FF may have been caused by the thicker TiO$_2$ layer, which may increase the
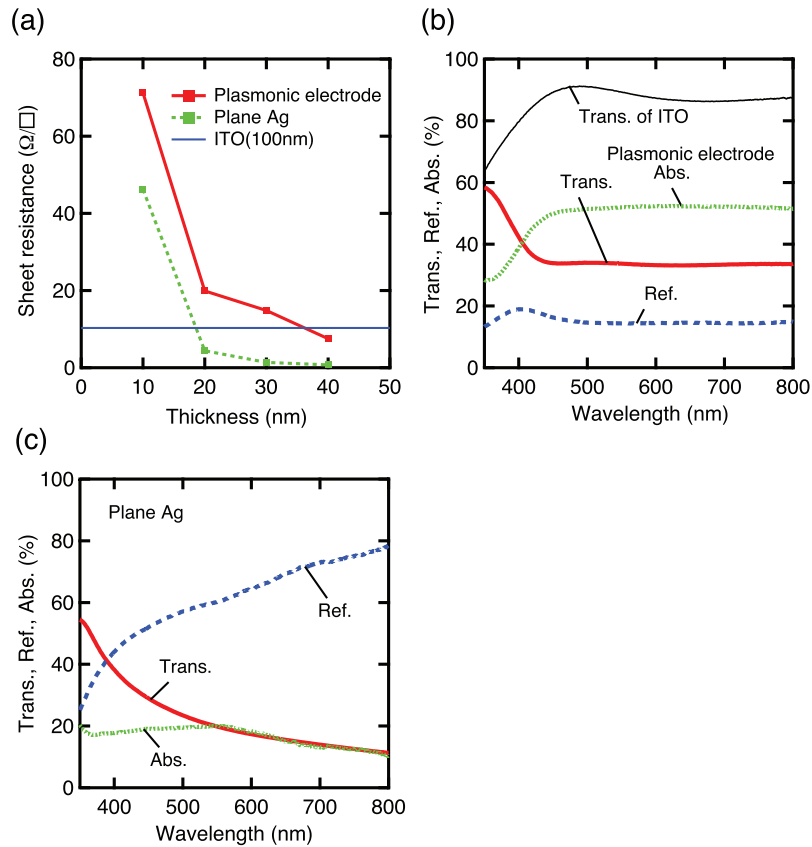
Figure 2. (a) The sheet resistance of the plasmonic electrodes and plane silver films against the film thickness. Transmission, reflection and absorption spectra of (b) a 30 nm thick plasmonic electrode and (c) a 30 nm thick plane silver film. The transmission spectrum of a 100 nm thick ITO electrode on a glass substrate is also shown in (b) for comparison.
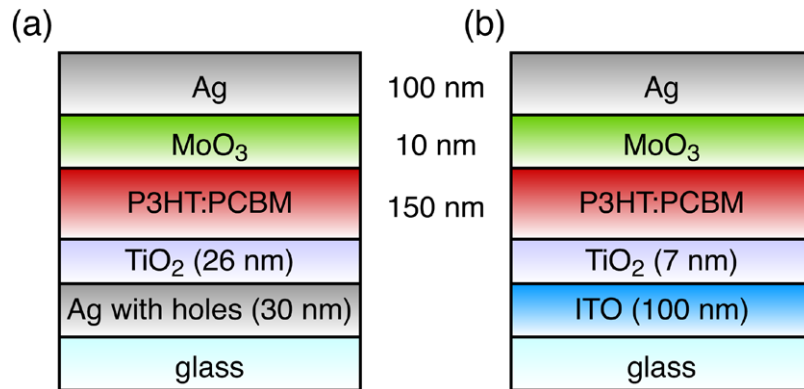
Figure 3. (a) Layer structure of plasmonic solar cells and (b) that of inverted solar cells.

shunt resistance. In the inverted solar cells, however, thicker TiO_2 layers only degraded their performance.

Figure 4(b) shows the measured incident photon to current efficiency (IPCE) spectra. The IPCE of the plasmonic solar cells, η_P, was higher than that of the inverted ones, η_I, around 400 nm and over 620 nm wavelength. The IPCEs were calculated for J_{sc} of the OSCs. Since J_{sc} of the plasmonic solar cells was lower than that of the inverted ones, η_P was also lower than η_I over most of the wavelength region. Figure 4(c) shows the absorption spectra of both solar cells. The absorption spectrum of the inverted solar cell is dominated by the absorption of P3HT:PCBM. The absorption of the plasmonic solar cells is higher than that of the inverted ones in the regions around 400 nm and over 610 nm, where the absorption by P3HT:PCBM is intrinsically weak but enhanced by the SPPs. In the other regions, the IPCE of the plasmonic solar cells was lower than that of the inverted ones. Since the lifetime of the SPP depends on the imaginary part of the permittivity of not only metals but also dielectric materials, the lifetime of the SPP in the regions where P3HT:PCBM exhibits high absorption is quite short. Thus, the SPPs contribute less to the absorption enhancement and the high surface reflection reduces the absorption in these regions.

(a)

(b)

(c)
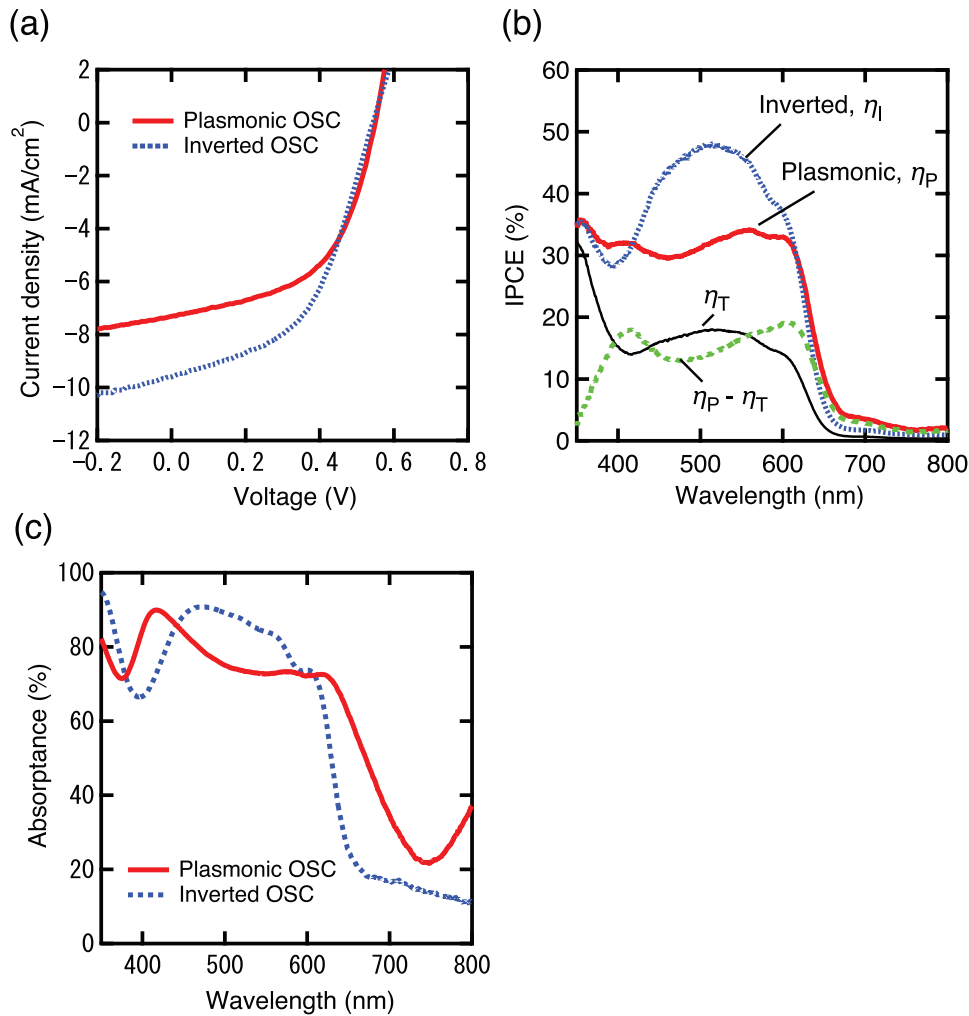
Figure 4. (a) Typical I–V curves of the plasmonic solar cell and the inverted solar cell under 1-SUN irradiation. (b) Typical incident photon to current efficiency (IPCE) spectra and (c) absorption spectra of the plasmonic solar cell and the inverted solar cell: η_P, plasmonic solar cell, η_I, inverted one, η_T, plasmonic solar cell only with the contribution of transmitted light and $\eta_P - \eta_T$, plasmonic solar cell only with the contribution of SPPs.

Hereafter, we estimate the contribution of the SPPs to the current generation in OSCs. Without SPP effects, only the light that passes through the plasmonic electrode contributes to the current generation. The contribution of the transmitted light on the IPCE of the plasmonic solar cells is estimated to be $\eta_T = \eta_I(T_{PL}/T_{ITO})$ (see figure 4(b)), where T_{ITO} and T_{PL} are the transmittances of the ITO film and the plasmonic electrode, respectively. Since the transmittance of the plasmonic electrode is much lower than that of ITO, η_T is also much lower than η_I. The rest, i.e. $\eta_P - \eta_T$ corresponds to the contribution of the SPPs (see figure 4(b)), which is comparable to that of the transmitted light and very wideband, as shown in figure 4(b). However, in the wavelength region shorter than 400 nm it is quite low because no SPPs can be supported by silver here.

5. Summary

We proposed a novel plasmonic electrode composed by a silver thin film with randomly perforated nanoholes 100 nm

in diameter. The perforation is done without any constraints, so the holes are both circular or of random shapes made by the connections of the holes. Such plasmonic electrodes can replace ITO ones in OSCs, leading to the advantages of flexibility and non-use of indium. Although the transmittance of the plasmonic electrode is 35%, much lower than that of ITO, the obtained PCE with plasmonic solar cells was comparable to that of the inverted solar cells. This is caused mainly by the contribution of SPPs and partly by the improvement of FF. The obtained IPCE of the plasmonic solar cells was higher than that of the standard ones around 400 nm and over 620 nm wavelength. This region corresponds to where the absorption of the active layer is weak. In this study, the diameter and the density of the holes in the plasmonic electrodes have not been optimised yet. The diameter and the density of the holes can be controlled by the diameter of the silica particles and their concentration in suspension, respectively. We expect that optimising these parameters will further improve the performance of the plasmonic solar cells, paving the way for next-generation flexible devices.

J. Phys. D: Appl. Phys. **49** (2016) 185106

K Takatori *et al*

Acknowledgment

References

[1] Li G, Zhu R and Yang Y 2012 *Nat. Photon.* **6** 153–61
[2] Li G, Shrotriya V, Huang J S, Yao Y, Moriarty T, Emery K and Yang Y 2005 *Nat. Mater.* **4** 864–88
[3] Nelson J 2002 *Curr. Opin. Solid State Mater. Sci.* **6** 87–95
[4] van de Lagemaat J, Barnes T M, Rumbles G, Shaheen S E, Coutts T J, Weeks C, Levitsky I, Peltola J and Glatkowski P 2006 *Appl. Phys. Lett.* **88** 233503
[5] Hecht D S, Hu L and Irvin G 2011 *Adv. Mater.* **23** 1482–513
[6] Cairns D R, Witte R P II, Sparacin D K, Sachsman S M, Paine D C, Crawford G P and Newton R R 2000 *Appl. Phys. Lett.* **76** 1425
[7] Sierros K A, Morris N J, Ramji K and Cairns D R 2009 *Thin Solid Films* **517** 2590–5
[8] Minami T and Miyata T 2008 *Thin Solid Films* **516** 1474–7
[9] Durkop T, Getty S A, Cobas E and Fuhrer M S 2004 *Nano Lett.* **4** 35–9
[10] Allen M J, Tung V C and Kaner R B 2010 *Chem. Rev.* **110** 132–45
[11] Novoselov K S, Geim A K, Morozov S V, Jiang D, Zhang Y, Dubonos S V, Grigorieva I V and Firsov A A 2004 *Science* **306** 666–9
[12] Wu J, Agrawal M, Becerril H A, Bao Z, Liu Z, Chen Y and Peumans P 2010 *ACS Nano* **4** 43–8
[13] Nair R R, Blake P, Grigorenko A N, Novoselov K S, Booth T J, Stauber T, Peres N M R and Geim A K 2008 *Science* **320** 1308
[14] Wu J, Becerril H A, Bao Z, Liu Z, Chen Y and Peumans P 2008 *Appl. Phys. Lett.* **92** 263302
[15] Pode R B, Lee C J, Moon D G and Han J I 2004 *Appl. Phys. Lett.* **84** 4614
[16] Ghosh D S, Martinez L, Giurgola S, Vergani P and Pruneri V 2009 *Opt. Lett.* **34** 325–7
[17] O'Connor B, Haughn C, An K H, Pipe K P and Shtein M 2008 *Appl. Phys. Lett.* **93** 223304
[18] Liu H D, Zhao Y P, Ramanath G, Murarka S P and Wang G C 2001 *Thin Solid Films* **384** 151–6
[19] Lindquist N C, Luhman W A, Oh S H and Holmes R J 2008 *Appl. Phys. Lett.* **93** 123308
[20] Kang M G, Xu T, Park H J, Luo X and Guo L J 2010 *Adv. Mater.* **22** 4378–83
[21] Luhman W A, Lee S H, Johnson T W, Holmes R J and Oh S H 2011 *Appl. Phys. Lett.* **99** 103306
[22] Chou S Y and Ding W 2013 *Opt. Express* **21** A60–76
[23] Reilly T H III, van de Lagemaat J, Tenent R C, Morfa A J and Rowlen K L 2008 *Appl. Phys. Lett.* **92** 243304
[24] Reilly T H III, Tenent R C, Barnes T M, Rowlen K L and van de Lagemaat J 2010 *ACS Nano* **4** 615–24
[25] Kang M G, Kim M S, Kim J and Guo L J 2008 *Adv. Mater.* **20** 4408–13
[26] Kang M G and Guo L J 2007 *J. Vac. Sci. Technol.* B **25** 2637–41
[27] Atwater H A and Polman A 2010 *Nat. Mater.* **9** 205–13
[28] Ferry V E, Munday J N and Atwater H A 2010 *Adv. Mater.* **22** 4794–808
[29] Hayashi S and Okamoto T 2012 *J. Phys. D: Appl. Phys.* **45** 433001
[30] Stec H M and Hatton R A 2013 *Adv. Energy Mater.* **3** 193–9
[31] Raether H 1988 *Surface Plasmons on Smooth and Rough Surfaces and on Gratings* (Berlin: Springer)